03,04

Proton conductivity of $LaZrO_{3.5}$ pyrochlore + $LaScO_3$ perovskite thin-film composite materials

© V.P. Gorelov, V.B. Balakireva

Institute of High-Temperature Electrochemistry, Ural Branch, Russian Academy of Sciences, Yekaterinburg, Russia

E-mail: gorelov@ihte.ru

Received April 30, 2025
Revised May 15, 2025
Accepted May 19, 2025

Disorder that occurs at the dissimilar phase interfaces in oxide composite materials is favorable for water adsorption, therefore, is also favorable for appearance of proton conductivity at these interfaces. High composite conductivity requires a developed network of phase interfaces implemented in thin films synthesized at low temperatures. Such thin-film materials may turn out to be promising proton electrolytes for solid oxide fuel cells designed for low-temperature operation.

$LaZrO_{3.5}$ pyrochlore + $LaScO_3$ perovskite composite materials in the form of films up to 250 nm in thickness served as a model object for investigation of this effect. The films were deposited onto ZrO_2 + 10 mol.% Y_2O_3 single-crystal substrates by spreading the measured amounts of alcoholic nitrate solutions and examined in the entire composition range from 0 to 100 % $LaScO_3$.

Conductivity measurements of the films using the impedance method in the 250−500 °C range proved that the maximum conductivity occurred in the 1:1 composite material in humid air. The effect was not available in dry air.

Keywords: oxide films, composite materials, perovskite $LaScO_3$, pyrochlore $La_2Zr_2O_7$, impedance, proton conductivity.

DOI: 10.61011/PSS.2025.06.61682.101-25

1. Introduction

Design of solid oxide fuel cells (SOFC) is a promising area of distributed generation development. High efficiency and low material consumption of SOFC may be achieved only in structures where film techniques are used, and such structures are being developed actively. General SOFC development trend is reducing the operating temperatures. For low temperatures (to 600 °C and lower), SOFCs with proton oxide electrolytes are promising and have fundamental advantages in these conditions compared with oxygen-containing electrolytes because activation energy of proton conductivity is much lower than that of oxygen conductivity. Moreover, electrode reaction activation energy is also lower in the case of proton electrolytes.

However, the prospects of creating proton electrolytes with high bulk conductivity don't seem promising for these conditions, therefore the intergranular conductivity effects are of interest for researchers due to the composite effect [1], in particular in films [2–4]. The composite effect is caused by the increase in two-phase sample conductivity by means of lateral (along the grain boundary) intergranular conductivity at the interface of two phases and occurs in the sample when the percolation threshold is reached. Therefore the maximum composite effect shall be observed for the volume phase ratio of 1:1. The greater the contribution of the lateral intergranular conductivity to the total conductivity of a material the more developed the interface network, therefore, the contribution will be higher in a fine-crystalline structure.

High disorder of noncoherent or semicoherent interfaces that is induced in case of contact between dissimilar phases is favorable for water adsorption, therefore, it is favorable for occurrence of proton conductivity along these interfaces [3]. The simplest method to form such film electrolytes is dip coating, where a substrate is immersed in a thermally decomposable salt solution. The dip coating method has no restrictions in the number of components, moreover, this film synthesis method may be conducted at low temperatures about 600−800 °C, thus, providing a nanograin film structure. Authors of [4] report that dense nanocrystalline oxide films may be used as electrolytes in electrochemical devices.

For investigation of the composite effect in proton conductivity, the proposed work selected a thin-film model system consisting of two co-existing fine-crystalline phases: $LaZrO_{3.5}$ pyrochlore + $LaScO_3$ perovskite. The above-mentioned compounds were not doped to avoid dopant release at the interfaces and to detect the influence of particularly interface disorder on proton conductivity.

2. Experiment procedure

The following precursors for film synthesis was used: $ZrO(NO_3)_2 \cdot 5H_2O$ (extra pure), La_2O_3 (LaO-D) and Sc_2O_3 (99.98 %). lanthanum and scandium oxides were

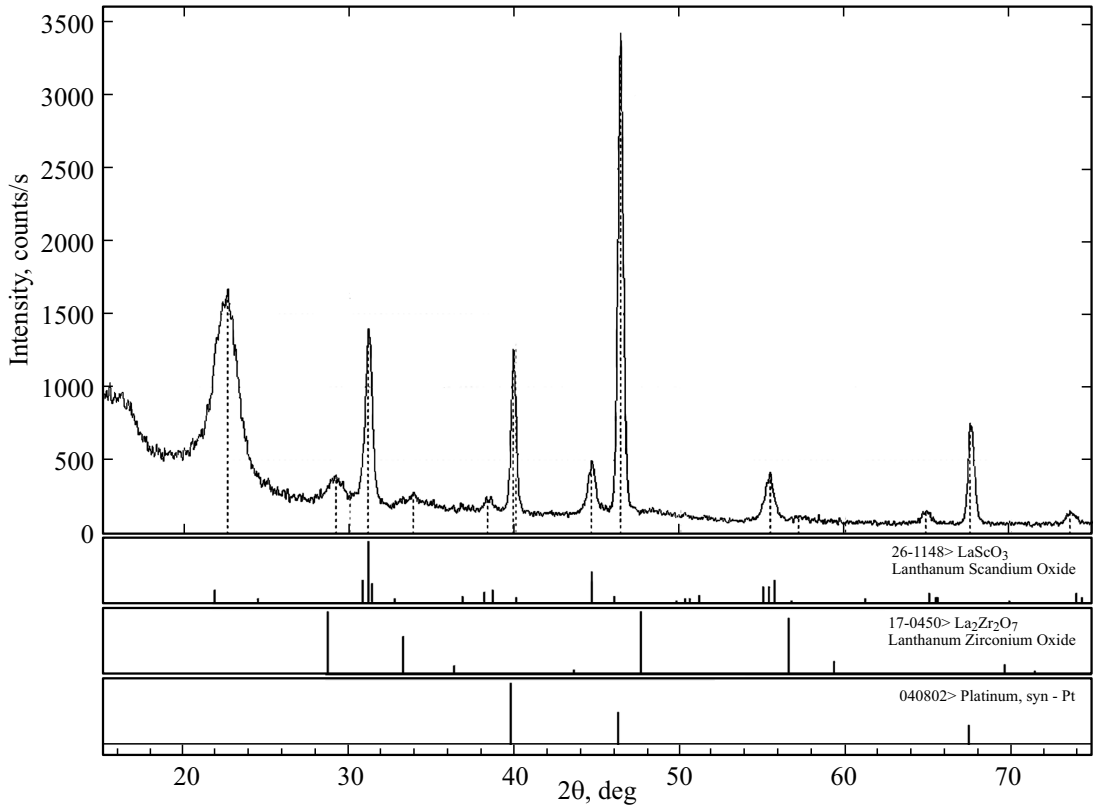

Figure 1. Diffraction pattern of the $0.5LaZrO_{3.5} + 0.5LaScO_3$ film synthesized at 850 °C on a platinum substrate. X-ray bar diagrams of Pt, $LaScO_3$ and $La_2Zr_2O_7$ are shown.

dissolved in nitric acid (chemically pure). Nitrate solutions in ethanol (solution concentrations about 0.5 mol.% with reference to oxides) were used as precursors for film synthesis. $ZrO_2 + 10$ mol.% Y_2O_3 (YSZ) single-crystal wafers served as substrates for film deposition. YSZ wafers oriented in the 111 plane had a diameter about 12 mm and a thickness about 1.5 mm. Final polishing of the wafers was conducted using diamond paste with a grain size of $0-1\mu$m.

Films were deposited by spreading the measured amount of titrated solution on the surface of an calcined single crystal. Final film thickness test was performed by the optical method using the LEF-3M ellipsometer. The films were deposited on both sides of the YSZ wafers, synthesis was conducted at 600 °C at a heating rate of 50 °C/h. Thermogravimetric analysis of the salt mixture combined with mass-spectrometry showed that this temperature was sufficient for full decomposition of salts.

To achieve the desired film thickness, the deposition process was repeated. Mean oxide film thickness per one application was about 30 nm. Final film thickness reached 250 nm. These samples were used for electric conductivity measurement.

In addition, films with a thickness about 120 nm were synthesized on a platinum substrate at 850 °C. They gave a more clear diffraction picture with narrow lines. Alcohol solutions poorly wet platinum, therefore the platinum surface was preliminary activated, for which it was wetted with a weak nitrate solution in white spirit and calcined.

X-ray diffraction analysis (XFA) of the films was performed in grazing beam at an incident angle of 1.5° on the Rigaku Dmax 2200 diffractometer in CuK_α radiation with monochromator. Results were evaluated using JCPDS database.

Scanning electron microscopy (SEM) was performed using the MIRA 3 LMU (TESCAN, Czech Republic) and JSM-5900LV (JEOL) microscopes.

Electric conductivity of films was measured by the impedance spectroscopy method (in the frequency range of $1-10^6$ Hz) using the Elins (Russia) impedancemeter at a signal amplitude of 30 mV. Measurements were performed using symmetrical cells with $Ag|f|YSZ|f|Ag$ electrodes, where f is the film to be studied. YSZ electrolyte prevents electrode short-circuit through possible film defects [5,6]. Silver electrodes were applied twice by coating with paste and baked at 550 °C during 0.5 h. Electric conductivity measurements were performed at 300–500 °C in humid and dry air. Film conductivity was calculated using the following equation:

$$\sigma = 2d[S(R_2 - R_1)]^{-1},$$

where d is the film thickness, S is the electrode area equal to the sample diameter, R_2 and R_1 are X-coordinate values corresponding to the right and left edge of the arc on the impedance spectrum corresponding to the film contribution.

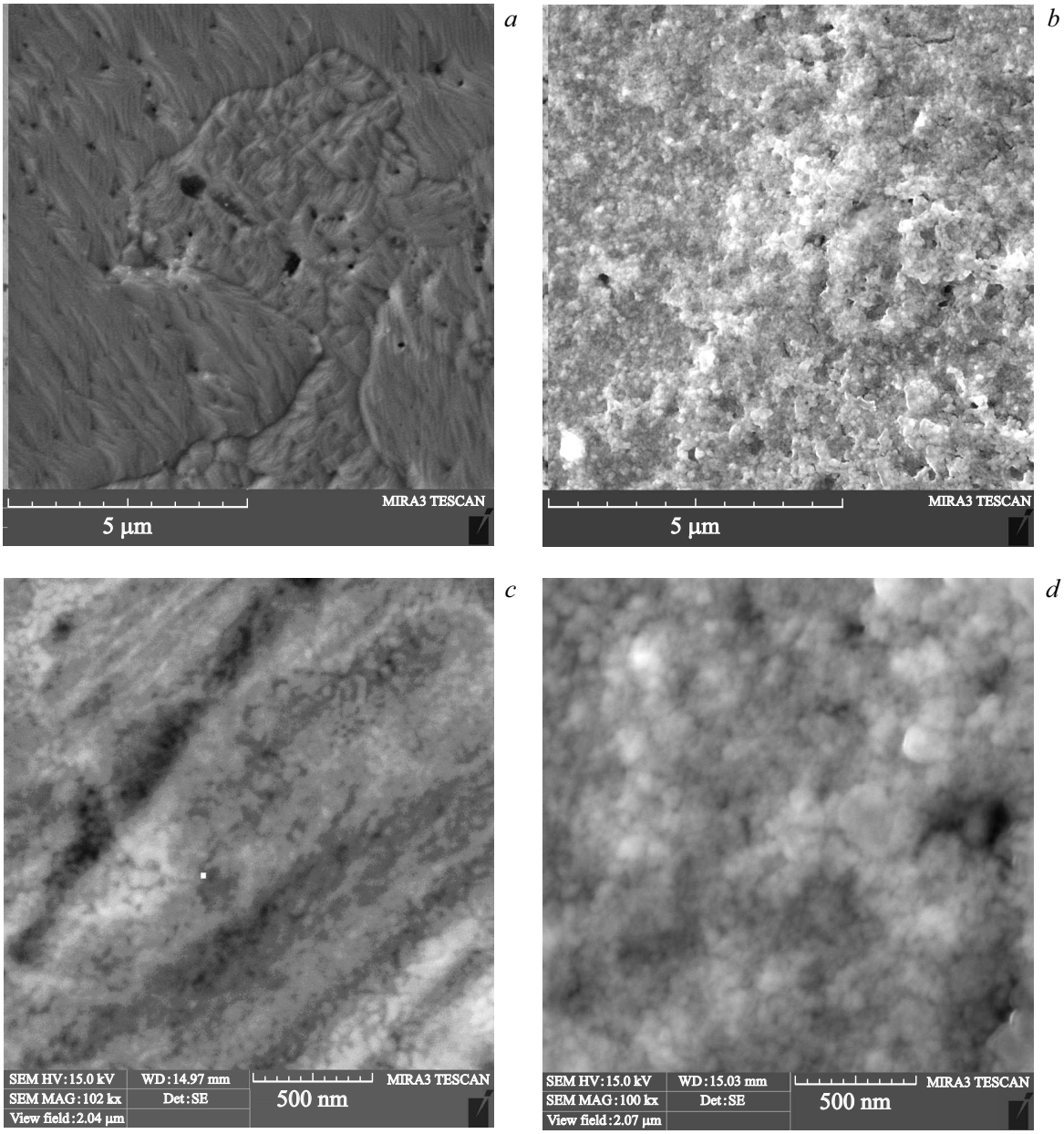

Figure 2. SEM images of the $LaZrO_{3.5}$ (*a, b*) and $LaScO_3$ (*c, d*) films on platinum: one film layer (*a, c*) and ten layers (*b, d*).

The required air humidity was provided by air circulation in a closed circuit containing a bubbler with controlled water temperature (23 °C). Dry atmosphere was provided by means of air circulation through a zeolite column (residual water steam pressure $pH_2O \approx 40$ Pa measured using the „Baikal-3M“ hygrometer).

3. Results and discussion

3.1. Film synthesis results

Films on platinum were glossy, transparent and changed their color from dark-blue to gold as the thickness increased. Films on YSZ single-crystal substrates were transparent, but colorless, suggesting that refractive indices of the film and substrate were close to each other.

Diffraction patterns of composite films synthesized at 850 °C (Figure 1) confirm that the pyrochlore, $LaZrO_{3.5}$ (LZ), and perovskite, $LaScO_3$ (LS), phase mixture was formed.

It is known [7,8] that there are no pyrochlore lines, if $LaZrO_{3.5}$ is synthesized via codeposition of hydroxides at temperatures up to 900 °C. Pyrochlore structure is not available in this case, there are only fluorite lines. Water left in the lattice prevents ordering. Appearance of low-temperature metastable phases initiated by the presence of water in rare-earth oxides was investigated in detail by Glushkova [9]. Synthesis at temperatures higher than

900 °C leads to water removal from oxide and formation of a pyrochlore structure. This is confirmed by neutron diffraction investigations [7]. However, film synthesis in our conditions leads to formation of pyrochlore (Figure 1).

The authors of [10] note low solubility of scandium dopant in ceramic $LaZr_{1-x}Sc_xO_{3.5}$ ($x = 0$, 0.05, 0.10, 0.15) samples synthesized at 1600 °C $LaScO_3$ phase occurred in samples with initial doping at $x = 0.05$ [10].

According to the SEM data, films cover the metallic platinum surface even after one application. Film crystals are oriented in accordance with the orientation of platinum grains whose boundaries are clearly seen. Lateral size of film grains reached 50–100 nm (Figure 2). Films synthesized at 600 °C on YSZ single-crystal substrates were X-ray amorphous, consequently, the crystallite size was about 5–10 nm.

After tenfold film application, orientation is not observed any longer and platinum grain boundaries cannot be seen (Figure 2, *b, d*).

3.2. Conductivity of undoped $LaScO_3$ and $LaZrO_3$ films

Utilization of YSZ single crystals that have no grain boundaries and appropriate response in the impedance spectrum as substrates simplifies data analysis considerably.

At low temperature (Figure 3, *a*), the impedance spectrum of the Ag|*f*|YSZ|*f*|Ag cell has a full arc going to the origin of coordinates, that is a response of the YSZ single crystal. A part of arc from the electrode process is observed in the low-frequency spectrum. This process can be fully seen at high temperatures, but then the response from the single crystal gets to be seen only partially (Figure 3, *b, c*).

A clear minimum is observed in the impedance spectrum between responses from the single crystal and electrode, when there is no film (Figure 3, *b*, curve *1*). When there is a film that separates the single crystal and electrode, an arc occurs in place of the minimum and is the response from the film (Figure 3). Corresponding values of the capacity C are given in Figure 3, *b, c*.

Substrate indifference was checked by comparing the conductivities of ten-layer $LaScO_3$ films synthesized on single crystals at 600 °C (during 10 h) and at 1100 °C (during 10 h). Measurements showed that conductivities of these films coincide at the activation energy equal to 1.44 ± 0.02 eV (Figure 4). This coincidence of conductivities confirms weak interaction between the LS film and YSZ substrate at 1100 °C, particularly at 600 °C. Moreover, it indicates that the synthesis reaction is completed at 600 °C. It is clear that grain boundaries in films synthesized at 600 and 1100 °C differ considerably and the conductivity coincidence is indicative of low grain boundary resistance in the undoped $LaScO_3$ samples. The latter has been also detected in the ceramic $LaScO_3$ samples [11].

Conductivity of the undoped $LaScO_3$ film in humid air is lower than in dry air (Figure 5) as for the bulk conductivity of the ceramic undoped $LaScO_3$ samples [12].

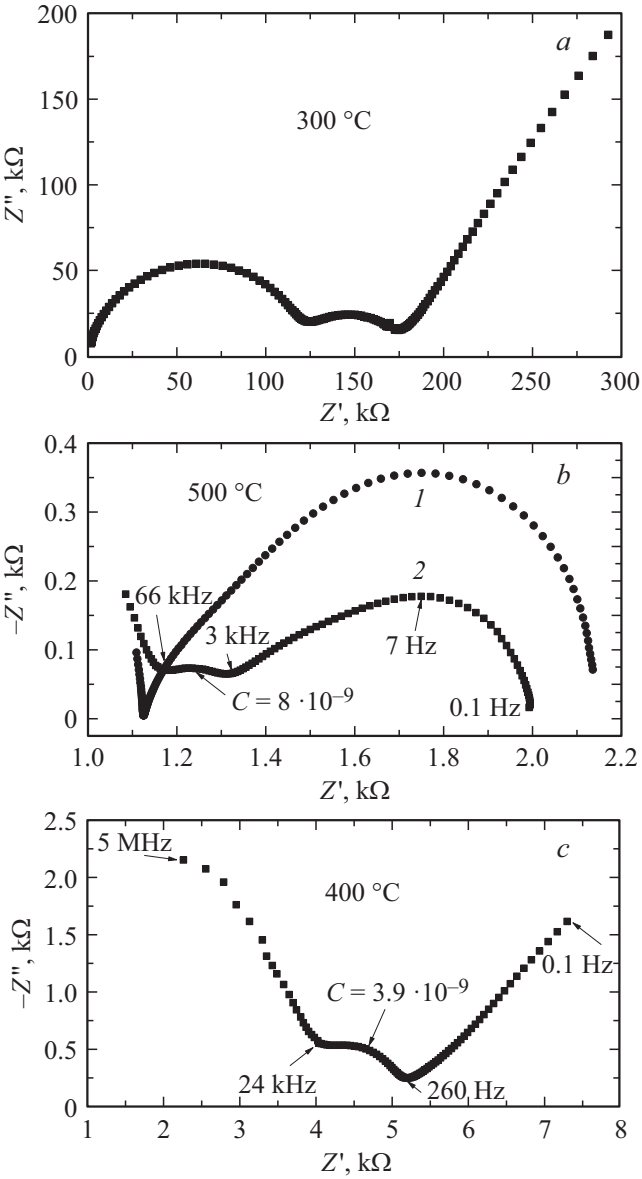

Figure 3. Impedance spectra of the Ag|*f*|YSZ|*f*|Ag cells: *a*) with LS film at 300 °C; *b*) without film (*1*) and with LS film (*2*) at 500 °C; *c*) with LZ film at 400 °C.

Bulk conductivity response of undoped $LaScO_3$ to humidity variation implies that there is high intrinsic disorder allowing water vapor to be dissolved in a considerable amount, for example, as a result of reaction (1) with the oxygen vacancies $V_O^{\bullet\bullet}$ or reaction (2) with participation of interstices $V_i^{\times}$:

$$H_2O + V_O^{\bullet\bullet} + O_O^{\times} = 2OH_O^{\bullet}, \quad (1)$$

$$H_2O + V_i^{\times} = (H_2O)_i^{\times}. \quad (2)$$

High solubility of $LaZrO_{3.5}$ in $LaScO_3$ (see below, Figure 6) and formation of interstitial oxygen during the reaction indicate higher probability of reaction (2). In any case, reactions (1) and (2) lead to a decrease in the p-type

conductivity that prevails in undoped $LaScO_3$ [11,12] due to a decrease oxygen solubility as a result of competing reactions (3) and (4):

$$1/2O_2 + V_O^{\bullet\bullet} = 2h^{\bullet} + O_O^{\times}, \quad (3)$$

$$1/2O_2 + V_i^{\times} = 2h^{\bullet} + O_i^{''}. \quad (4)$$

Unlike orthorhombic LS, conductivity of undoped cubic LZ is essentially independent of air humidity (Figure 5). Therefore, water vapor weakly interacts both with the LZ volume, despite the presence of large anion interstices, and with grain boundaries. Consequently, neither bulk nor lateral intergranular proton conductivity take place in LZ. This conclusion agrees with the data concerning low solubility of water vapor even in p-type doped pyrochlores, for example, in $La_{1-x}Ca_xZrO_{3.5-\alpha}$ [13] and $La_2(Zr_{0.9}Y_{0.1})_2O_{7-\delta}$ [10].

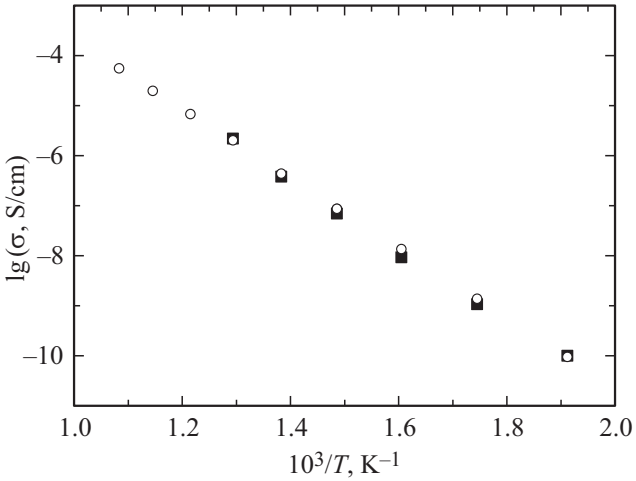

Figure 4. Conductivity polytherms in dry air of the $LaScO_3$ films synthesized on YSZ single crystals at 600 °C (filled squares) and 1100 °C (open circles).

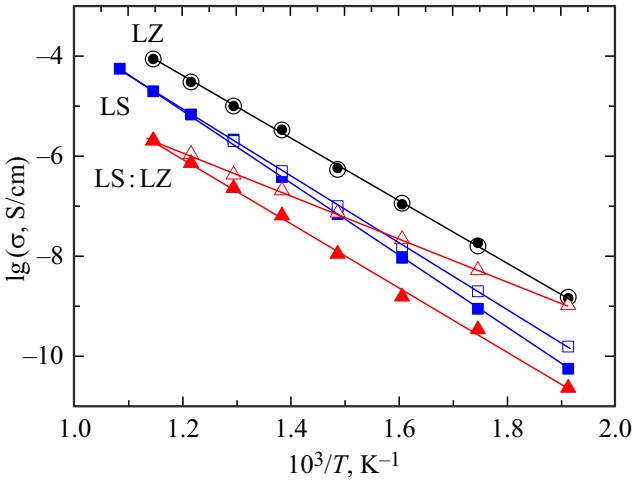

Figure 5. Conductivity polytherms of the $LaScO_3$ films (squares), $LaZrO_{3.5}$ films (circles) and 1:1 mixture thereof (triangles) in dry air (filled symbols) and humid air (open symbols).

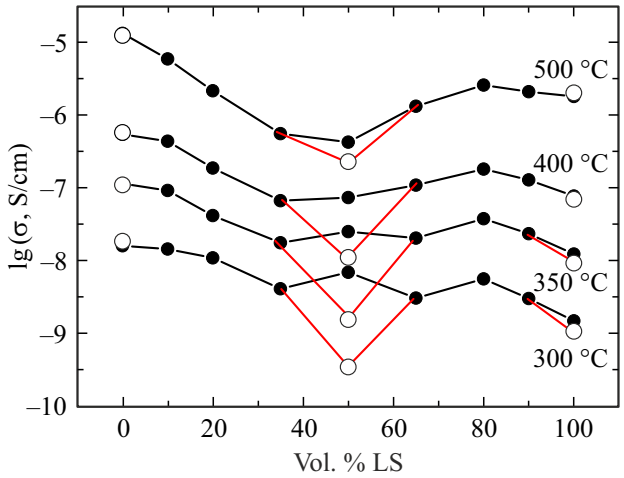

Figure 6. Conductivity isotherms of composite $LaZrO_{3.5}$+ $LaScO_3$ films in humid air (filled circles) and dry air (open circles).

According to [10], water vapor solubility (in damp argon, $pH_2O = 0.0312$ atm) even at 200 and 400 °C was max. 1/3 of the nominally possible value. Such behavior is probably explained by full order of oxygen vacancies in the LZ structure up to 1070 K according to the neutron diffraction data [14]. Nevertheless, the conductivity of the cubic $LaZrO_{3.5}$ film is an order of magnitude as high as that of the orthorhombic $LaScO_3$ film, despite the high disorder of the latter (Figure 6).

3.3. Conductivity of composite $LaZrO_{3.5}$ + $LaScO_3$ films

Basically, the synthesis of composite $LaZrO_{3.5} + LaScO_3$ materials shall give a mixture of their solutions, rather than a mixture of pure compounds, due to the scandium and zirconium cation exchange. p-type-scandium-doped $LaZr_{1-x}Sc_xO_{3.5-x/2}$ solid solution occurs on the basis of pyrochlore, and n-type zirconium-doped $LaSc_{1-y}Zr_yO_{3+y/2}$ solid solution occurs on the basis of perovskite. To separate the mutual doping effect from the composite effect, films with nine compositions were synthesized in the entire volume ratio range from 0 to 100 % LS and conductivity was measured.

As mentioned above, Han et al. [10] report that scandium solubility in $LaZr_{1-x}Sc_xO_{3.5-x/2}$ at 1600 °C was not higher than $x = 0.05$. In this work, the synthesis was conducted at a temperature lower by 1000 °C and the scandium solubility shall be much lower. Actually, p-type scandium doping of pyrochlore didn't cause any increase in pyrochlore conductivity (Figure 6).

Unlike $LaZrO_{3.5}$, $LaScO_3$ dissolves a considerable amount of zirconium, consequently, a maximum occurs in the conductivity isotherms when the LS concentration is 80 vol.% (Figure 6). n-type zirconium doping of $LaSc_{1-y}Zr_yO_{3+y/2}$ leads to formation of interstitial oxygen that block water vapor dissolution.

A deep minimum is observed in the two-phase region in dry air for 1:1 composition (Figure 6). A considerable increase in conductivity is observed in humid air in the same expected composite effect region. The higher the temperature the greater the increase.

3.4. Results and discussion

Conductivity of the samples in the LZ + LS two-phase region shall not be lower than the conductivity of each of the phases. If this is observed (Figure 6), then the decrease is caused by the presence of grain boundary resistance. In a two-phase sample, there are two types of grain boundaries — homophase boundaries (between the grains of the same phase) and heterophase boundaries (between the grains of different phases). And since the conductivity of composite LZ + LS materials reaches its maximum at the volume phase ratio of 1:1, then it is apparent that it is heterophase boundaries that are responsible for the decrease in conductivity. The most probable reason for this is the appearance of a barrier layer for both electron carriers and oxygen ions when p-type doped $LaZr_{1-x}Sc_xO_{3.5-x/2}$ contacts with n-type doped $LaSc_{1-y}Zr_yO_{3+y/2}$. Even occurrence of low proton conductivity in pyrochlore in humid air will not change the situation because the n-type doped LS has no proton conductivity and this transfer will be blocked in contact with LZ. Therefore, the positive composite effect observed in humid air in the region of LZ:LS = 1:1 may take place only due to the lateral intergranular proton conductivity resulting from water adsorption at disordered heterophase boundaries. Beyond the 1:1 composite ratio region, there is no lateral conductivity of films, which indicates that current lines are interrupted, i. e. a percolation threshold is observed (Figure 6). A considerable decrease in the composite effect at 500 °C indicates that the effect is implemented due to physical adsorption of water at the boundaries.

4. Conclusion

The impedance method was used to examine the lateral conductivity of $LaZrO_{3.5}$ pyrochlore + $LaScO_3$ perovskite, thin-film composite materials deposited by the deep coating method onto the YSZ single-crystal substrates in the composition range from 0 to 100 % $LaScO_3$. The studies conducted in dry air ($pH_2O \approx 40$ Pa) and humid air ($pH_2O \approx 2500$ Pa) within the temperature range of 250–500 °C found that:

- interaction between initial undoped composite phases during the synthesis leads to weak p-type scandium doping of $LaZrO_{3.5}$ and n-type zirconium doping of $LaSc_{1-x}Zr_xO_3$ that reaches $x \geq 0.2$;
- a barrier that occurs at the heterophase boundaries between the doped $LaZrO_{3.5}$ and $LaScO_3$ phases hinders the transfer of all current carriers through the interface, which induces a deep conductivity minimum in the two-phase region in dry air;
- in humid air against the background of the specified conductivity minimum, a maximum is observed in the $LaZrO_{3.5}$:$LaScO_3$ = 1:1 region, which indicates that there is a composite effect for the lateral (along heterophase grain boundaries) proton conductivity caused by water vapor adsorption at the grain boundaries. The effect may be used as the basis of low-temperature proton electrolyte synthesis.

Acknowledgments

Equipment provided by the Shared Access Center „Composition of Compounds“) of Institute of High Temperature Electrochemistry, Ural Branch of RAS, was used. The authors are grateful to A.A. Pankratov for undertaking the electronic microscopy.

Conflict of interest

The authors declare that they have no conflict of interest.

References

[1] N.F. Uvarov. Kompozitsionnye tverdye elektrolity. Izd-vo SO RAN, Novosibirsk (2008). p. 258. (in Russian).
[2] B. Zhang. Mater. Sci. Technol. **33**, *15*, 1728 (2017).
[3] Y. Meng, J. Gao, Z. Zhao, J. Amoroso, J. Tong, K.S. Brinkman. J. Mater. Sci. **54**, 9291 (2019).
[4] J. Gu, L. Jiang, S.A. Ismail, H. Guo, A.D. Han. Adv. Mater. Interfaces **10**, 2201764 (2023).
[5] L.A. Dunyushkina, S.V. Smirnov, S.V. Plaksin, V.M. Kuimov, V.P. Gorelov. Ionics **19**, 1715 (2013).
[6] L.A. Dunyushkina, S.V. Smirnov, V.M. Kuimov, V.P. Gorelov. Int. J. Hydrog. Energy **39**, 18385 (2014).
[7] P.S. Savchenkov, E.A. Goremychkin, V.V. Popov, B.L. Shapir, P.A. Borisova, A.A. Yastrebtsev, B.R. Gaynanov, M.P. Krasnov, A.P. Menushenkov, P.A. Alekseev. JETP Lett. **108**, *8*, 532 (2018).
[8] H. Chen, Ya. Gao, H. Luo, Sh. Tao. J. Therm. Spray Technol. **20**, *6*, 1201 (2011).
[9] V.B. Glushkova Polimorfizm okislov reddkozemel'nykh elementov. Nauka, L. (1967), p. 133. (in Russian).
[10] A.D. Han, K. Kojima, M. Majima, T. Uda. J. Electrochem. Soc. **161**, *10*, 977 (2014).
[11] V.P. Gorelov, A.Yu. Stroeva. Russ. J. Electrochem. **48**, *10*, 949 (2012).
[12] A.Yu. Stroeva, V.P. Gorelov. Russ. J. Electrochem. **48**, *11*, 1079 (2012).
[13] E.P. Antonova, A.S. Farlenkov, E.S. Tropin, V.A. Eremin, A.V. Khodimchuk, M.V. Ananyev. Solid State Ion. **306**, 112 (2017).
[14] T. Hagiwara, K. Nomura, H. Yamamura. Solid State Ion. **262**, 551 (2014).

Translated by E.Ilinskaya